

# Temperature Dependence of Ultrasonic Backscattered Energy in Motion-Compensated Images

R. Martin Arthur, Jason W. Trobaugh, William L. Straube and Eduardo G. Moros

**Abstract**— Noninvasive temperature imaging would enhance the ability to uniformly heat tumors at therapeutic levels. Ultrasound is an attractive modality for this purpose. Previously, we predicted monotonic changes in backscattered energy (CBE) of ultrasound with temperature for certain sub-wavelength scatterers. We also measured CBE values similar to our predictions in bovine liver, turkey breast, and pork muscle in 1D. Those measurements were corrected manually for changes in the axial position of echo signals with temperature. To investigate the effect of temperature on CBE in 2D, we imaged 1-cm thick samples of bovine liver, turkey breast, and pork muscle during heating in a water bath. Images were formed by a Terason 2000 imager with a 7 MHz linear probe. Employing RF signals permitted the use of cross-correlation as a similarity measure for automatic tracking of feature displacement as a function of temperature. Feature displacement across the specimen was non-uniform with typical total displacements of 0.5 mm in both axial and lateral directions. Apparent movement in eight image regions in each specimen was tracked from 37 to 50°C in 0.5°C steps. Envelopes of motion-compensated image regions were found with the Hilbert transform then smoothed with a 3x3 running average filter before forming the backscattered energy at each pixel. Our measure of CBE compared means of both the positive and negative changes in the BE images. CBE was monotonic and differed by about 4 dB at 50°C from its value at 37°C. Relatively noise-free CBE curves from tissue volumes of less than 1 cm<sup>3</sup> supports the use of CBE for temperature estimation.

**Keywords**— diagnostic ultrasound, hyperthermia, noninvasive thermometry

## I. INTRODUCTION

**H**YPERTHERMIA is a cancer treatment in which tumors are elevated to cytotoxic temperatures (41-45°C) in order to aid in their control [1], [2]. A major limitation of thermal therapies, however, is the lack of detailed thermal information available to guide and assess the therapy. In clinical procedures, temperatures are measured invasively and therefore only sparse measurements can be made.

To meet the capability of present and forthcoming heating technologies, a clinically useful method is needed to accurately (0.5°C) measure three-dimensional (3D) temperature distributions with at least 1 cm<sup>3</sup> spatial resolution. A noninvasive method for rapid volumetric determination of temperature distribution during treatment would facilitate targeted heating of tumors at therapeutic levels in patients receiving hyperthermia treatment [3]. The required accuracy and spatial resolution may be achievable

with magnetic resonance imaging, but MRI is expensive and interfacing the technology with heating devices may be difficult [4].

Ultrasound is a non-ionizing, convenient, and inexpensive modality with relatively simple signal processing requirements. These attributes make it an attractive method to use for temperature estimation if an ultrasonic parameter, which is dependent on temperature, can be found, measured, and calibrated.

Previously, we made 1D measurements of changes in backscattered ultrasonic energy (CBE) with temperature in abattoir specimens of bovine liver, turkey breast, and pork muscle that were consistent with the predictions of our model for CBE from tissue inhomogeneities in the form of sub-wavelength scatterers [5], [6]. Predicted and measured changes in backscattered energy were nearly monotonic with temperature and could serve as the basis for a calibration protocol. An important limitation of the CBE method, however, is that CBE is dependent on changes in the apparent location of scattering regions that occur with changes in speed of sound and tissue motion [7].

Our previous 1D measurements of CBE required segmenting and tracking echoes from individual scattering regions [6]. In this study we measured the change in backscattered energy in conventional diagnostic ultrasonic images at temperatures ranging from 37 to 50°C. In order to compensate for apparent motion of tissue features with temperature, we developed and evaluated algorithms for tracking tissue regions that showed displacement of image features during tissue heating. As in our earlier 1D studies, the CBE in motion-compensated images tracked monotonically with temperature, which is encouraging for the use of ultrasound as a thermometer.

## II. ULTRASONIC MEASUREMENT OF TEMPERATURE

Methods for using ultrasound as a non-invasive thermometer fall into three categories: 1) Those based on the measurement of the acoustic attenuation coefficient, 2) Those based on echo shifts due to thermal expansion and changes in speed of sound (SOS), and 3) Our approach, which exploits changes in backscattered energy (CBE) from a single backscatter view measured with standard equipment.

The primary ultrasonic parameter examined for its dependence on temperature in early work was speed of sound (SOS) [8], [9], [10]. In these initial studies investigators tried to obtain SOS maps of the medium from which to

R. M. Arthur and J. W. Trobaugh are with the Department of Electrical and Systems Engineering, Washington University School of Engineering. e-mail: rma@ese.wustl.edu

W. L. Straube and E. G. Moros are with the Department of Radiation Oncology, Washington University School of Medicine

infer temperature distributions. This approach, however, has never been instituted clinically [11]. Perhaps this approach has not been implemented because in order to measure SOS, it is necessary to measure both distance and time, to image an identifiable target from two directions, or to use a crossed-beam (multiple beams) method [12]. Such measurement is further complicated by the fact that ultrasonic windows do not always exist *in vivo* to allowinsonification of a region of interest from two views. Another problem is that the temperature dependence of SOS differs depending on the tissue type, e.g. whether tissue has high water or fat content.

#### A. Attenuation Coefficient

Damianou and coworkers investigated the temperature dependence of ultrasonic attenuation and absorption in soft tissues [13]. They found that attenuation was highly dependent on temperature above 50°C. Ribault and coworkers [14] also looked at the effect of temperature rise on frequency-dependent attenuation and found that tissue damage (lesion formation) caused a change in attenuation in porcine liver *in vitro* at temperatures above 50°C. This effect was found by looking at the backscattered signal over the volume of the lesion, and comparing the power received before and after high intensity focused ultrasound (HIFU). Other investigators have observed similar effects in the past [15].

In the hyperthermia range the attenuation coefficient change is small. In bovine liver at 7 MHz that change is about  $0.1 \text{ cm}^{-1}$  [16]. The temperature range in which attenuation effects are readily measured ( $> 50^\circ\text{C}$ ), however, is not suitable for moderate-temperature hyperthermia because temperatures for this therapy do not exceed  $45^\circ\text{C}$ .

#### B. Echo Shift

The use of echo shifts has received the most attention in the last decade as a method for estimating temperature. Although this approach has been successful in calibrated, homogeneous tissue phantoms, it has not as yet been reduced to a practical *in vivo* ultrasonic thermometer. By tracking scattering volumes and measuring the time shift of received echoes, investigators have been able to predict the temperature from a region of interest both theoretically and experimentally.

Seip and Ebbini initially presented a technique in which tissue temperature was inferred from the change in resonant frequencies of echo signals using an autoregressive model [17]. This technique required initial knowledge of the average scatterer spacing. For this reason it may be difficult to use *in vivo*. In later investigations by Ebbini and coworkers tracking echo shifts from scattering volumes was shown to be promising, as was the work of other investigators looking at echo shifts [18]. Maass-Moreno and coworkers investigated the ability to predict temperature in HIFU therapy from echo shifts in turkey breast muscle [19], [20]. They found that results were consistent with their theoretical predictions. Sun and Ying have also found some success in being able to predict temperatures using

time-gated echo shifts, but they acknowledge the difficulty of using this method for general temperature monitoring because prior knowledge of both SOS and thermal expansion coefficients is necessary [3]. Like attenuation-based methods, most of these efforts have been geared towards HIFU therapy and may not be suitable for monitoring of moderate-temperature hyperthermia.

In ultrasonic imaging, techniques for motion estimation, estimation of the displacement between two image regions comprise an active field of research [21], [22], [23], [24], [25] and have been used successfully for elasticity imaging, phase aberration correction, blood velocity estimation, and other applications. In these areas, motion estimation is typically called speckle tracking or time-delay estimation. Work based on exploiting thermal effects that induce tissue strain has primarily been aimed at guiding focused ultrasound therapies rather than at accurate estimation of temperatures [26], [27], [28], [29].

#### C. Backscattered Energy

We modeled the energy in the back scattered signal from a small volume due to an interrogating ultrasonic wave [5]. According to that model, the change in backscattered energy due to temperature from 37 to  $50^\circ\text{C}$  was primarily dependent on the changes in SOS and density of the medium compared to their values in sub-wavelength inhomogeneities (scatterers) within the medium. Our predicted change in backscattered energy at any temperature  $T$  with respect to its value at some reference temperature  $T_R$  is

$$CBE(T) = \frac{\alpha(T_R)}{\alpha(T)} \frac{\eta(T)}{\eta(T_R)} \frac{[1 - e^{-2\alpha(T)x}]}{[1 - e^{-2\alpha(T_R)x}]}, \quad (1)$$

where, as functions of temperature,  $\alpha(T)$  is the attenuation within the tissue volume and  $\eta(T)$  is the backscatter coefficient of the tissue volume. Distance  $x$  is the path length in the tissue volume. We inferred the temperature dependence of the backscatter coefficient from the scattering cross section of a sub-wavelength scatterer [30], [31]. Neglecting the effect of the small change in the wavenumber ( $< 1.5\%$ ) with temperature, we assumed [5]

$$\frac{\eta(T)}{\eta(T_R)} = \frac{\left( \frac{\rho_m c(T)_m^2 - \rho_s c(T)_s^2}{\rho_s c(T)_s^2} \right)^2 + \frac{1}{3} \left( \frac{3\rho_s - 3\rho_m}{2\rho_s + \rho_m} \right)^2}{\left( \frac{\rho_m c(T_R)_m^2 - \rho_s c(T_R)_s^2}{\rho_s c(T_R)_s^2} \right)^2 + \frac{1}{3} \left( \frac{3\rho_s - 3\rho_m}{2\rho_s + \rho_m} \right)^2}, \quad (2)$$

where  $\rho$  and  $c$  are the density and speed of sound of the scatterer  $s$  and medium  $m$ . This expression applies to conditions where the wavelength  $\lambda$  is larger than  $2\pi a$ , where  $a$  is the radius of the scatterer. Assuming a speed of sound of  $1.5 \text{ mm}/\mu\text{s}$  and a frequency of  $7.5 \text{ MHz}$ ,  $\lambda$  is  $0.2 \text{ mm}$ , which means that Eq. 1 using Eq. 2 applies to scatterers smaller than  $30 \mu\text{m}$ .

We predicted CBE from individual scatterers of as much as 5 dB over the temperature range from 37 to  $50^\circ\text{C}$ . Furthermore, backscattered energy can increase or decrease depending on the type of inhomogeneity that caused the

scattering. Model predictions were calculated from second and third order polynomial descriptions of the attenuation and speed of sound as a function of temperature for the medium, a lipid scatterer, and an aqueous scatterer. These polynomials were based on measured data from the literature. Values for density and predictions about CBE sensitivity to density changes is covered in detail in the description of the model [5].

### III. METHODS

To test the use of the change in backscattered energy as a possible parameter for temperature estimation, phased-array images of *in vitro* tissue specimens were taken as a function of temperature. CBE was calculated, after compensation for the apparent motion of scattering regions. We also tested for non-thermal effects on tissue and for changes in the experimental apparatus with temperature.

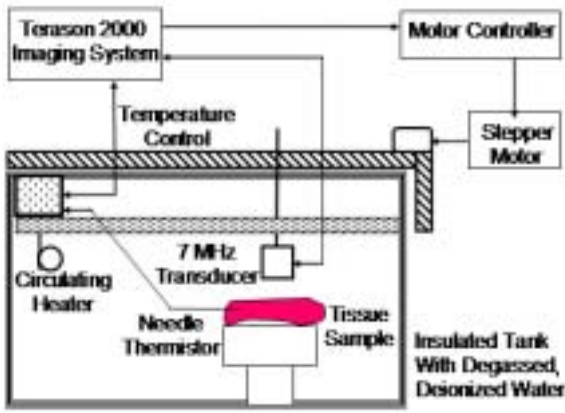


Fig. 1. Configuration for automatic image measurement from tissue samples. Deionized and degassed water was heated to equilibrium under control of the imaging system.

#### A. Measurement of Backscattered Images

Measurements of backscattered energy as a function of temperature were made with the experimental configuration depicted in Figure 1. Tissue samples were heated in an insulated tank that was filled with deionized water, which had been degassed by vacuum pumping in an appropriate vessel. Experiment te149 on bovine liver (see Results), the third of the 7 experiments presented in this paper, was run in 0.9% saline to check for possible effects of edema on CBE. Because results were similar to those for the first two experiments, the saline medium was not used again.

We measured CBE from 37 to 50°C in order to encompass the hyperthermia treatment range, i.e., for temperatures up to around 42°C. In addition to providing context for hyperthermia temperatures, the 37 to 50°C range matched our previous theoretical study of the dependence of CBE on the backscatter coefficient of sub-wavelength scatterers. That study was based on data in the literature available only up to 50°C. For temperatures above 50°C we expect attenuation effects to become important, as noted previously in Section II.

Images were formed by a Terason 2000 system (Teratech Corp.) with a 128-element, 7 MHz linear probe (model 10L5) focused at 4.5 cm, the center of the tissue specimen. A typical image is shown in Figure 2. The accompanying movie shows apparent motion of the specimen due to heating from 37 to 50°C.

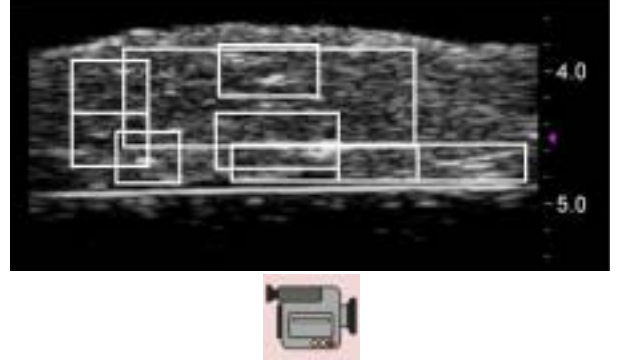


Fig. 2. Ultrasonic image of bovine liver. Focal zone of the 7 MHz transducer was at 4.5 cm (arrowhead marker). Superimposed boxes indicate regions studied. The movie shows apparent motion due to heating from 37 to 50°C. [Media-Movie 1](#)

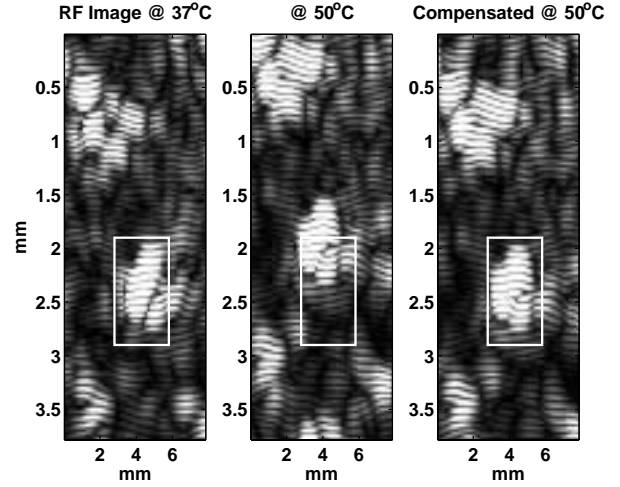


Fig. 3. Radio-frequency images of bovine liver at 37°C (left) and 50°C (center & right). Alternating bands indicate positive and negative excursions of the RF signal. Features in the fixed, highlighted region appear to have moved both axially and laterally at 50°C compared to positions at 37°C. Motion compensation to correct for apparent motion of image features was applied to the image at 50°C (right).

The notebook computer that the imaging system was based upon was also used to control tissue heating. Desired tissue temperature was set by controlling a circulating heater via a serial link using a custom Matlab (Mathworks, Inc.) routine. The temperature in the tissue was monitored by a thermometer, which used an indwelling needle RTD thermistor. That temperature was reported to the Matlab routine, which turned off the pump when the desired temperature was reached. Control was then switched to the Terason 2000 to acquire and save an image frame or



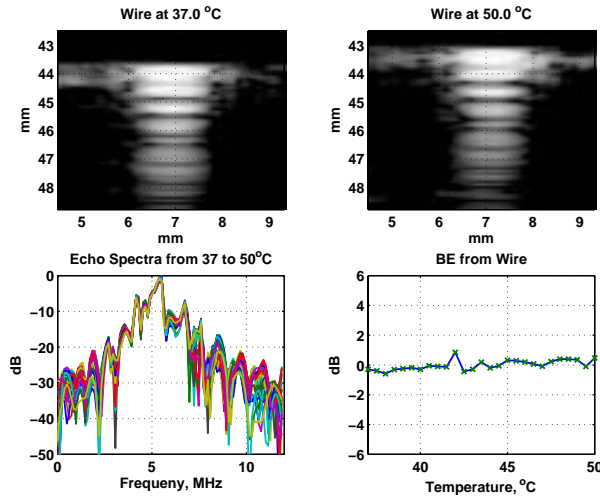


Fig. 4. Effect of temperature on a test object. Upper panels) Images of a stainless steel wire in the AIUM 100 mm test object at 37°C and 50°C. Apparent motion towards the transducer with an increase in temperature is seen. Lower left) Magnitude spectra of the radio frequency echo from the center of the wire image from 37 to 50°C with no motion compensation. Lower right) The backscattered energy from the wire from 37 to 50°C on the same scale used for CBE in tissue (see the Results).

loop. The process was repeated in 0.5°C increments over the 37 to 50°C range. The acquisition process, which took about 45 minutes, was automated. All keystrokes needed to switch between Matlab and the Terason 2000 program, and to save image files were administered using AutoIT keystroke-emulation software (hiddensoft.com).

### B. Tracking and Compensating for Apparent Motion

Previously we manually compensated for apparent axial motion in 1D radio-frequency (RF) images before calculating CBE [6]. Apparent motion with temperature in an RF image of an image region is shown in Figure 3. The movie accompanying Figure 2 shows the apparent motion of the whole specimen with heating.

For a given region, motion was compensated for by first estimating the displacement of features from one temperature measurement to the next, then transforming the second image by the measured displacement. Employing RF signals from the Terason 2000 (courtesy Teratech Corp.) permitted the use of cross-correlation as a similarity measure for automatic tracking of feature displacement as a function of temperature.

To estimate feature displacement, the cross-correlation between images at adjacent temperatures was maximized. Estimation was implemented using a combination of optimization and image resampling functions available in Matlab to eliminate dependence on the spatial sampling period of the image. This method was applied to eight regions within each tissue sample as indicated in Figure 2.

### C. Backscattered Energy in Motion-Compensated Images

Once apparent tissue motion was accounted for, change in backscattered energy was calculated over the measured

temperature range. Envelopes of motion-compensated image regions were found with the Hilbert transform then smoothed with a 3x3 running average filter. Values were squared to determine the backscattered energy at each pixel. The backscattered energy image at 37°C was typically used as the reference for CBE images at each 0.5°C step.

### D. Non-thermal and Unwanted Thermal Effects

We also tested our system under conditions for which we expected to see no change in backscattered energy. We measured CBE in bovine liver over the time required for an experiment, but without heating, to determine the magnitude of non-thermal effects. CBE values of  $< \pm 0.2$  dB were typical of the changes seen over 80 minutes, twice the approximate duration of an experiment.

The AIUM test object [32] was used to evaluate thermal effects on the Terason 2000 transducer itself. CBE from a wire in the test object over the time of a typical experiment was  $< \pm 0.1$  dB at a constant temperature. The images of a stainless steel wire in the AIUM 100 mm test object at 37°C and 50°C in Figure 4 show apparent motion towards the transducer with an increase in temperature. The apparent axial motion over that range was accounted for by the expected change in the speed of sound in water. Also shown in Figure 4 are the magnitude spectra of the radio frequency echo from the center of the wire image in 0.5 °C steps from 37 to 50°C with no motion compensation. The spectrum of the backscattered signal does not change significantly over the measured temperature range. Finally, backscattered energy from the wire from 37 to 50°C is plotted in Figure 4 on the same scale used for CBE in tissue (see Results). These small changes have been neglected in the results presented.

## IV. RESULTS

To investigate the effect of temperature on changes in backscattered energy in 2D, we imaged 1-cm thick samples of bovine liver, turkey breast, and pork muscle during heating in a water bath from 37 to 50°C. Images were formed by a Terason 2000 imager with a 7 MHz linear probe.

As tissue specimens were heated, features in fixed-frame images appeared to move. That motion was tracked and compensated for as described in Section III. The energy at each pixel in motion-compensated images was calculated and compared to its value at 37°C. The change in backscattered energy was nearly monotonic with temperature.

### A. Apparent Motion of Scattering Regions

Apparent tissue motion in both axial and lateral directions was analyzed in eight regions (Figure 2) in each of seven tissue specimens. As shown in Figure 5 tissue appears to move closer to the transducer in all but two of the liver specimens, which is consistent with the increase in the speed of sound in the water path between the tissue and transducer.

There is also a non-uniform component to tissue motion as indicated by the lateral changes. That tissue-dependent

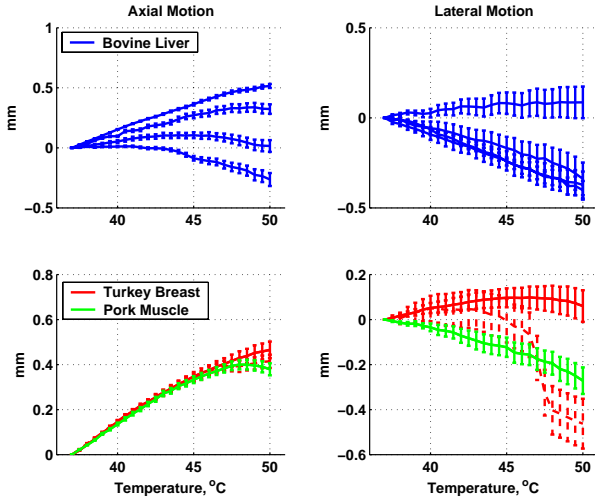


Fig. 5. Apparent motion of tissue in the axial and lateral dimensions due to temperature. Each plot is the mean of motion in eight regions  $\pm$  the standard error of the mean for each tissue specimen. Results from four bovine liver samples are shown in the upper panels, for two turkey breast and one pork muscle samples in the lower panels. In one turkey specimen (solid line), tissue fibers were parallel to the array of transducer elements. In the other (dashed line), striations were perpendicular to the array. Motion depicted in Figure 3 was quantified using cross correlation of RF signals as seen in that figure.

component also contributed to the axial motion, as seen particularly at temperatures above  $47^{\circ}\text{C}$ . Note too the difference in the apparent lateral motion in the two specimens of turkey breast. In the one which exhibited nearly constant lateral motion, tissue fibers were parallel to the array of transducer elements. In the one which showed a change of several tenths of a millimeter near  $47^{\circ}\text{C}$ , striations were perpendicular to the array.

The maximum apparent motion across all specimens was about 0.5 mm in both the axial and lateral directions. This finding means that on average tissue movement was  $< 20 \mu\text{m}$  per  $0.5^{\circ}\text{C}$  step. This small change is consistent with visual observation of apparent motion and is a range over which the motion tracking and compensation methods functioned well.

### B. Change in Backscattered Energy in Images

After compensating for apparent motion, the change in backscattered energy at each pixel over each image region in all tissue specimens was calculated with respect to a reference temperature. Figure 6 shows four images of CBE with respect to backscattered energy at  $37^{\circ}\text{C}$  for one bovine liver sample. The accompanying movie shows CBE from 37 to  $50^{\circ}\text{C}$  in  $0.5^{\circ}\text{C}$  steps. The image at the reference temperature was always zero dB at all pixels by our definition of CBE. For some regions the CBE was positive for others it was negative as temperature increased. This kind of change was predicted by our model of the CBE for a single scatterer, depending on its density and speed of sound [5].

The means of the positive- and negative-valued pixels

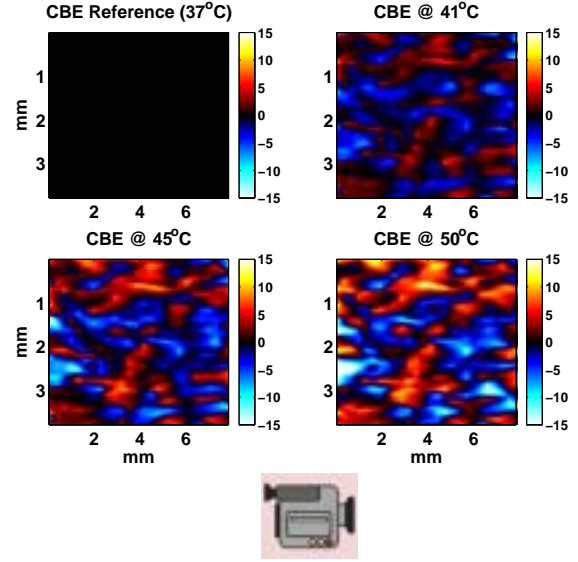


Fig. 6. CBE in RF images of bovine liver from 37 to  $50^{\circ}\text{C}$  after compensation for apparent motion. All images were referred to the CBE image at  $37^{\circ}\text{C}$ . The CBE scale is in dB and is symmetric about 0 dB (black). Motion tracking was applied to the central region of the image. The resulting translations were applied to the entire image region. The movie shows CBE from 37 to  $50^{\circ}\text{C}$  in  $0.5^{\circ}\text{C}$  steps. **Media-Movie 2**

in the CBE images from eight image regions in all tissue specimens is plotted in Figure 7. Means of both positive and negative CBE varied nearly monotonically by about 4 dB. The means  $\pm$  the standard error of the mean across the eight image regions for each tissue specimen of Figure 7, along with our previous prediction for the CBE from a single sub-wavelength scatterer with varying density and speed of sound are shown in Figure 8 [5].

The means from pixels with positive and negative relative backscattered energy changed monotonically. The match of measured CBE with our previous predictions of CBE may help explain its behavior in different tissues and build confidence in its application for ultrasonic thermometry. A single measure from CBE images, however, may be more useful for temperature estimation. Figure 9 shows the standard deviation of measured CBE over the same eight regions of BE images in each of the four specimens of bovine liver, two of turkey breast, and one of pork muscle analyzed for Figure 7. This figure compares the standard deviation of CBE in images to our previous measurements in 1D from specimens of bovine liver, turkey breast, and pork muscle [6]. The results using automatic analysis of images from a phased array in this study and those from manual segmentation of echo signals using a circular piston in the previous study are consistent [6].

## V. DISCUSSION

Analysis of ultrasonic images taken in  $0.5^{\circ}\text{C}$  steps for the temperature range from 37 to  $50^{\circ}\text{C}$  showed apparent motion in both the lateral and axial directions. This motion was compensated for by using a cross correlation technique that maximized the correlation at adjacent temper-

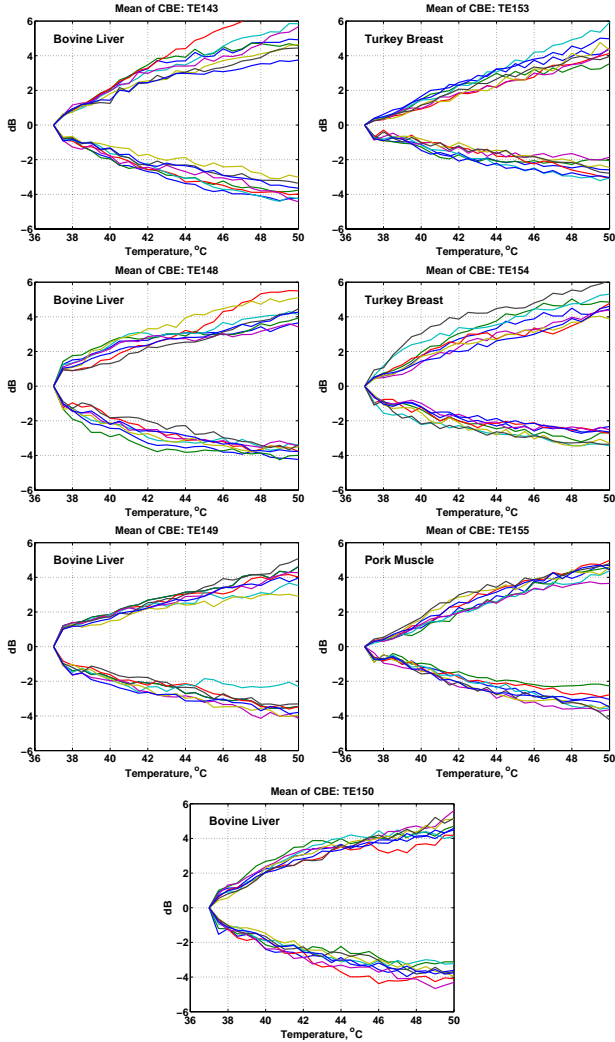


Fig. 7. Means of CBE for the positive and negative excursions in eight regions of interest for each of four samples of bovine liver, two of turkey breast, and one of pork muscle. The eight regions of interest for the liver specimen TE143 are shown in Figure 2.

atures to track feature displacement. After compensation for apparent axial and lateral movement of image features during heating, image regions showed changes in backscattered energy over the 37 to 50°C temperature range, which were clearly distinct from changes due to movement.

In this study we found rigid transformations for arbitrary image regions and applied them to those or slightly larger regions. These overlapping regions generally covered the image of each tissue specimen as seen in Figure 2. Our intent was to test the robustness of our motion-tracking approach and to elicit the behavior of CBE with temperature in different types of tissue, not to calibrate CBE for temperature estimation.

Ultimately, we plan to develop region tracking methods to estimate and compensate for the non-rigid deformations in image volumes acquired over changing temperatures. The ability to apply a non-rigid deformation to images of a tissue volume is an important step toward clinical application of ultrasonic temperature imaging based on changes in

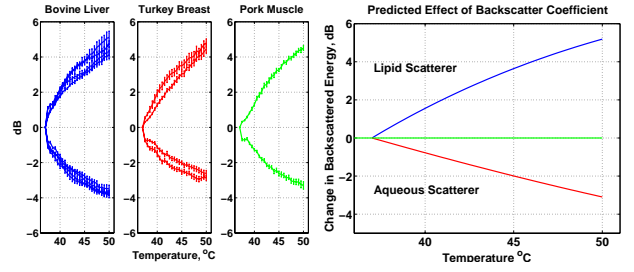


Fig. 8. Means of measured CBE in positive and negative regions of BE images in four specimens of bovine liver, two of turkey breast, and one of pork muscle (left). The error bar is the standard error of the mean estimated from eight regions of interest in each of the tissue specimens shown in Figure 7. Predicted CBE for single, sub-wavelength lipid and aqueous scatterers in an aqueous medium from our previous study [5] (right).

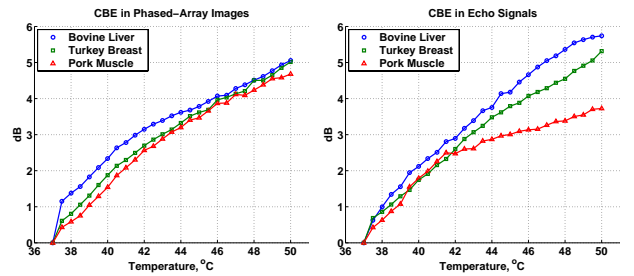


Fig. 9. Standard deviation of measured CBE over eight regions of BE images in each of four specimens of bovine liver, two of turkey breast, and one of pork muscle (left). Standard deviation of measured CBE in 1D from specimens of bovine liver, turkey breast, and pork muscle reported previously [6] (right).

backscattered energy. Such a development is critical to determining limitations on temperature accuracy and spatial resolution with CBE-based temperature estimation.

After motion compensation, the backscattered energy relative to the baseline at 37°C was analyzed at each pixel. Analysis showed both positive and negative excursions in the relative backscattered energy similar to what we had seen previously in the 1-D case [5]. These positive and negative excursions tracked nearly monotonically with temperature in the 37 to 50°C range, as seen in the plot for each specimen given in Figure 8. That figure also contains our predictions for CBE from lipid and aqueous sub-wavelength scatterers in an aqueous medium. Our predictions, however, were based on analyses of a single scatterer. We are working on simulating the expected CBE from random collections of scatterers to help us understand the effects of multiple scatterers on CBE. These simulations will also be used to study the effect of image noise on CBE performance.

Our findings of CBE behavior in images here and previously in 1D echo signals are quite similar (see Figure 9) [6]. One reason for that consistency is that the effect of the correction for apparent lateral motion may be small. If so, correction for apparent motion in elevation will be even smaller because for the Terason 2000 the elevation beam width at our focal zone was five times wider than



the lateral beam width. We have conducted preliminary experiments in 3D by taking seven 2D images separated by 0.6 mm in elevation at each temperature. We applied our motion detection and correction methods to a region in the resulting 3D volume then made movies of slices in elevation. As expected the dominant motion was in the axial direction. The apparent motion encountered in elevation was much smaller than the beam width in elevation, so that the percentage of scatterers that move in or out of the beam in elevation is expected to be smaller than the percentage in the lateral direction. Motion within a wide beam will change the backscattered energy less than that in a narrow beam. Thus, we expect CBE to support temperature estimation in 3D.

Another observation from Figure 9 is that the effect of noise on CBE may be greater in images than in our 1D measurements. This effect is seen at 37.5°C, where for liver in particular, CBE in images is about twice the value it was in 1D, even though the maximum CBE, at 50°C, was about 0.5 dB greater in 1D. The effect of motion artifact, which would increase CBE, is reduced in 2D because lateral motion is accounted for, but noise susceptibility may be increased. Every pixel, independent of its signal strength, was used in the 2D calculation of CBE, whereas signal-to-noise values were enhanced in 1D by segmentation of strong echo signals.

Future work includes refinement of the efficiency and accuracy of methods for tracking apparent tissue motion with temperature and investigation of other methods to statistically analyze the dependence of CBE on temperature in 3D in the presence of noise. Even so, the results from this study already support the use of backscattered ultrasonic energy as a modality for noninvasive thermometry and are consistent with theoretical expectations and previous findings.

## VI. CONCLUSIONS

The change in backscattered energy in motion-compensated images from a phased-array system was measured from 37 to 50°C in specimens of bovine liver, turkey breast, and pork muscle. Cross-correlation was used as a similarity measure for automatic tracking of feature displacement as a function of temperature. Maximum feature displacement across the specimen was about 0.5 mm in both the axial and lateral directions. This displacement was reached in 26 0.5°C steps over the temperature range. The small typical displacement from temperature to temperature was easily handled using the cross-correlation approach. CBE in motion-compensated images was nearly monotonic with a maximum change of 4-5 dB. The results from this study are consistent with our theoretical predictions and our previous findings in 1D.

Our approach has the advantage that it depends on tissue inhomogeneity. That dependence makes calibration difficult, but once done we expect the move to *in vivo* situations to be easier than it has been for time-of-flight or SOS methods. *In vitro* success of CBE temperature estimation based on 3D tracking and compensation for apparent mo-

tion of image features could serve as the foundation for the eventual generation of 3D temperature maps in soft tissue in a noninvasive, convenient, and low-cost way in clinical hyperthermia.

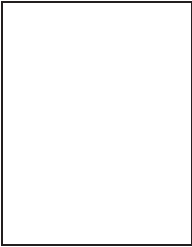
## VII. ACKNOWLEDGMENTS

This work was supported in part by NIH grant R21-CA90531 from the National Cancer Institute and by the Wilkinson Trust at Washington University in St. Louis.

## REFERENCES

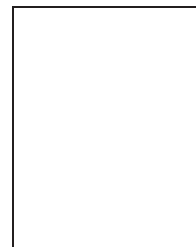
- [1] MW Dewhurst, L Prosnitz, D Thrall, D Prescott, S Cleff, C Charles, J Macfall, G Rosner, T Samulski, E Gillette, and S LaRue, "Hyperthermic treatment of malignant diseases: Current status and a view toward the future," *Seminars in Oncology*, vol. 24, pp. 616-625, 1997.
- [2] RJ Myerson, EG Moros, and JL Roti-Roti, "Hyperthermia," in *Principles and Practice of Radiation Oncology*, CA Perez and LW Brady, Eds., chapter 24, pp. 637-683. Lippincott-Raven, Philadelphia, third edition, 1998.
- [3] Z Sun and H Ying, "A multi-gate time-of-flight technique for estimation of temperature distribution in heated tissue: theory and computer simulation," *Ultrasonics*, vol. 37, pp. 107-122, 1999.
- [4] D Carter, J MacFall, S Clegg S, X Wan, D Prescott, H Charles, and T Samulski, "Magnetic resonance thermometry during hyperthermia for human high-grade sarcoma," *Int J Radiat Oncol Biol Phys*, vol. 40, pp. 815-822, 1998.
- [5] WL Straube and RM Arthur, "Theoretical estimation of the temperature dependence of backscattered ultrasonic power for noninvasive thermometry," *Ultrasound in Med And Biol*, vol. 20, pp. 915-922, 1994.
- [6] RM Arthur, WL Straube, JD Starman, and EG Moros, "Noninvasive temperature estimation based on the energy of backscattered ultrasound," *Medical Physics*, vol. 30, pp. 1021-1029, 2003.
- [7] RM Arthur, JW Trobaugh, WL Straube, EG Moros, and S Sangkatumvong, "Temperature dependence of ultrasonic backscattered energy in images compensated for tissue motion," in *Proceedings of the 2003 International IEEE Ultrasonics Symposium*. 2003, vol. No 03CH37476C, pp. 990-993, IEEE Press.
- [8] T Bowen, WG Connor, RL Nasoni, AE Pifer, and RR Sholes, "Measurement of the temperature dependence of the velocity of ultrasound in soft tissues," in *Ultrasonic Tissue Characterization II*, M Linzer, Ed. National Bureau of Standards, 1979, vol. Spec Publ 525, pp. 57-61, US Government Printing Office.
- [9] B Rajagopalan, JF Greenleaf, PJ Thomas, SA Johnson, and RC Bahn, "Variation of acoustic speed with temperature in various excised human tissues studied by ultrasound computerized tomography," in *Ultrasonic Tissue Characterization II*, M Linzer, Ed. National Bureau of Standards, 1979, vol. Spec Publ 525, pp. 227-233, U S Government Printing Office.
- [10] O Prakash, M Fabbri, M Drocourt, JM Escanyé, C Marchal, ML Gaulard, and J Robert, "Hyperthermia induction and its measurement using ultrasound," in *Proceedings of IEEE Symposium on Ultrasonics*. 1980, vol. 80CH1689-9, pp. 1063-1066, IEEE Press.
- [11] SA Johnson, DA Christensen, CC Johnson, JF Greenleaf, and B Rajagopalan, "Non-intrusive measurement of microwave and ultrasound-induced hyperthermia by acoustic temperature tomography," in *Proceedings of IEEE Symposium on Ultrasonics*. 1977, vol. 77CH1264-1 SU, pp. 977-982, IEEE Press.
- [12] J Ophir, "Estimation of the speed of ultrasound propagation in biological tissues: A beam-tracking method," *IEEE Trans on UFFC*, vol. UFFC-33, no. 4, pp. 359-368, July 1986.
- [13] CA Damianou, NT Sanghvi, FJ Fry, and R Maass-Moreno, "Dependence of ultrasonic attenuation and absorption in dog soft tissues on temperature and thermal dose," *J Acoust Soc Am*, vol. 102, pp. 628-634, 1997.
- [14] M Ribault, J Chapelon, D Cathignol, and A Gelet, "Differential attenuation imaging for the characterization of high intensity focused ultrasound lesions," *Ultrasonic Imaging*, vol. 20, pp. 160-177, 1998.
- [15] TC Robinson and PP Lele, "An analysis of lesion development in the brain and in plastics by high intensity focused ultrasound

- at low-megahertz frequencies," *J Acoust Soc Am*, vol. 5, pp. 1333–1351, 1972.
- [16] JC Bamber and CR Hill, "Ultrasonic attenuation and propagation speed in mammalian tissues as a function of temperature," *Ultrasound in Med and Biol*, vol. 5, pp. 149–157, 1979.
  - [17] R Seip and ES Ebbini, "Noninvasive estimation of tissue temperature response to heating fields using diagnostic ultrasound," *IEEE Trans on Biomed Engr*, vol. 42, pp. 828–839, 1995.
  - [18] Ebbini E Simon C, VanBaren P, "Two-dimensional temperature estimation using diagnostic ultrasound," *IEEE Trans on UFFC*, vol. 45, pp. 1088–1099, 1998.
  - [19] R Maass-Moreno and CA Damianou, "Noninvasive temperature estimation in tissue via ultrasound echo-shifts part i analytical model," *J Acoust Soc Am*, vol. 100, pp. 2514–2521, 1996.
  - [20] Sanghvi NT Maass-Moreno R, Damianou CA, "Noninvasive temperature estimation in tissue via ultrasound echo-shifts part ii in vitro study," *J Acoust Soc Am*, vol. 100, pp. 2522–2530, 1996.
  - [21] Goshtasby A, "Image registration by local approximation methods," *Image and Vision Computing*, vol. 6, pp. 255–261, 1988.
  - [22] Christensen GE, Joshi SC, and Miller MI, "Volumetric transformations of brain anatomy," *IEEE Trans on Med Imaging*, vol. 16, pp. 864–877, 1999.
  - [23] MA Lubinski, SY Emelianov, and M O'Donnell, "Speckle tracking methods for ultrasonic elasticity imaging using short-time correlation," *IEEE Trans on Ultrasonics, Ferroelectrics, and Frequency Control*, vol. 46, pp. 82–96, 1999.
  - [24] Fitzpatrick JM, Hill DLG, and Maurer CR, "Image registration," in *Handbook of Medical Imaging*, M Sonka and JM Fitzpatrick, Eds., Bellingham, Washington, 2000, vol. 2 Medical Image Processing and Analysis, pp. 447–513, SPIE The International Society for Optical Engineering.
  - [25] Viola FV and Walker WF, "A comparison of the performance of time-delay estimators in medical ultrasound," *IEEE Trans on Ultrasonics, Ferroelectrics, and Frequency Control*, vol. 50, pp. 392–401, 2003.
  - [26] NR Miller, JC Bamber, and PM Meaney, "Fundamental limitations of noninvasive temperature imaging by means of ultrasound echo strain estimation," *Ultrasound in Med & Biol*, vol. 28, no. 10, pp. 1319–1333, 2002.
  - [27] F L Lizzi, R Muratore, CX Deng, JA Ketterling, SK Alam, S Mikaelian, and A Kalisz, "Radiation-force technique to monitor lesions during ultrasonic therapy," *Ultrasound in Med & Biol*, vol. 29, no. 11, pp. 1593–u1605, 2003.
  - [28] W Liu, U Techavipoo, T Varghese, JA Zagzebski, Q Chen, and Jr F T Lee, "Elastographic versus x-ray ct imaging of radio frequency ablation coagulations: An in vitro study," *Med Phys*, vol. 31, no. 6, pp. 1322–1332, 2004.
  - [29] NR Miller, JC Bamber, and GR Ter Haar, "Imaging of temperature-induced echo strain: Preliminary in vitro study to assess feasibility for guiding focused ultrasound surgery," *Ultrasound in Med & Biol*, vol. 30, no. 3, pp. 345–u356, 2004.
  - [30] KK Shung, MB Smith, and B Tsui, *Principles of Medical Imaging*, Academic Press, San Diego, CA, 1992, pp 90–99.
  - [31] PM Morse and KU Ingard, *Theoretical Acoustics*, McGraw-Hill, New York, 1968, p 427.
  - [32] Erikson K R, Carson P L, and H F Stewart, "Field evaluation of the aium standard 100 mm test object," *Ultrasound in Medicine*, vol. 2, pp. 445–451, 1976.

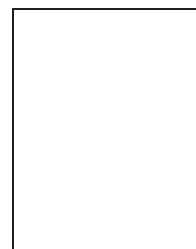


**R. Martin Arthur** was born in Houston, TX, on November 13, 1940. He received the B.A., B.S., and M.S. degrees in electrical engineering from Rice University, Houston, TX in 1962, 1963, and 1964, respectively. He received the Ph.D. degree in biomedical engineering from the University of Pennsylvania in 1968. Following postdoctoral work in auditory neurophysiology from 1969 to 1970 at Washington University, he joined the faculty there. He was an Assistant Professor of Electrical Engineering (1970–1975), Associate Professor of Electrical Engineering (1975–1983), and Professor of Electrical Engineering (1983–Present). At Washington University, he was also a Research Associate of the Biomedical Computer Laboratory from 1973 to 1987, Director of

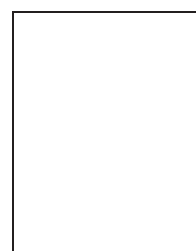
the Clinical Engineering Program from 1975 to 1980, is currently a Professor of Biomedical Engineering and Interim Chairman of the Department of Electrical and Systems Engineering. His current research interests include forward and inverse electrocardiology in the assessment of arrhythmia risk and synthetic-focus methods for image improvement and tissue characterization using medical ultrasound.



**Jason W. Trobaugh** (M'93) was born in Fort Leavenworth, Kansas on May 1, 1969. He earned the B.S. and M.S. degrees in electrical engineering from Washington University in St. Louis in 1991 and 1993, respectively. From 1993 to 1996 he was a research associate at Washington University. In 1996 he joined the Electronic Systems and Signals Research Laboratory of Washington University, where he completed the D.Sc. degree in electrical engineering in 2000. From 1996 to 2000, he also worked with the Surgical Navigation Technologies division of Medtronic, Inc. His research interests are in the fields of model-based image analysis, probabilistic image models, and treatment guidance applications for ultrasonic imaging.



**William L. Straube** earned a bachelors degree in Nuclear Engineering from the University of Illinois in 1983. While working in the Department of Radiology/Mallinckrodt Institute of Radiology at Washington University he earned his Masters Degree in Electrical Engineering in 1991. Currently he is a Research Associate Professor of Radiation Oncology in the Department of Radiation Oncology at Washington University Medical School.



**Eduardo G. Moros** was born in Caracas, Venezuela. He was conferred the B.S., M.S. and Ph.D. degrees in Mechanical Engineering at the University of Arizona, Tucson, Arizona, in 1984, 1987 and 1990, respectively, the latter two with minors in Electrical Engineering. He performed his graduate research at the Department of Radiation Oncology, Arizona Health Sciences Center, Arizona Cancer Center, working primarily on the development and in vitro and in vivo evaluation of bioheat transfer and ultrasound models for Thermoradiotherapy treatment planning applications. In July of 1991, Dr. Moros joined the faculty of Washington University Medical School as an Assistant Professor of Radiology (Radiation Oncology Center, Mallinckrodt Institute of Radiology, St. Louis, Missouri), where he was the Chief of Clinical Hyperthermia Physics for 14 years. While at Washington University, Dr. Moros led and collaborated in various externally funded research and development projects in Thermotherapy, Radiologic Physics, Biomedical Engineering and Bioelectromagnetics. In 2001, he was named the Head of the Physics Research Section of the newly formed Department of Radiation Oncology. He was promoted to Associate Professor with Tenure in 1999 and Full Professor on January 1, 2005. In August of 2005, Dr. Moros accepted the position of Director of the Division of Radiation Physics and Informatics in the Department of Radiation Oncology at the University of Arkansas for Medical Sciences, Little Rock, AR, where he is now overseeing clinical operations and expanding research activities. His main interest has been to facilitate the translation of basic scientific findings to clinical application by developing specialized physics/engineering models and systems. Currently, he is particularly interested in the application of molecular imaging/therapy for the treatment of cancer with heat and radiation.